



Deep learning methods for modeling infrasound transmission loss in the middle atmosphere

JANELA CAMEIJO Alice^{1,4}, LE PICHON Alexis¹,
SKLAB Youcef², ARIB Souhila³, AKNINE Samir⁴

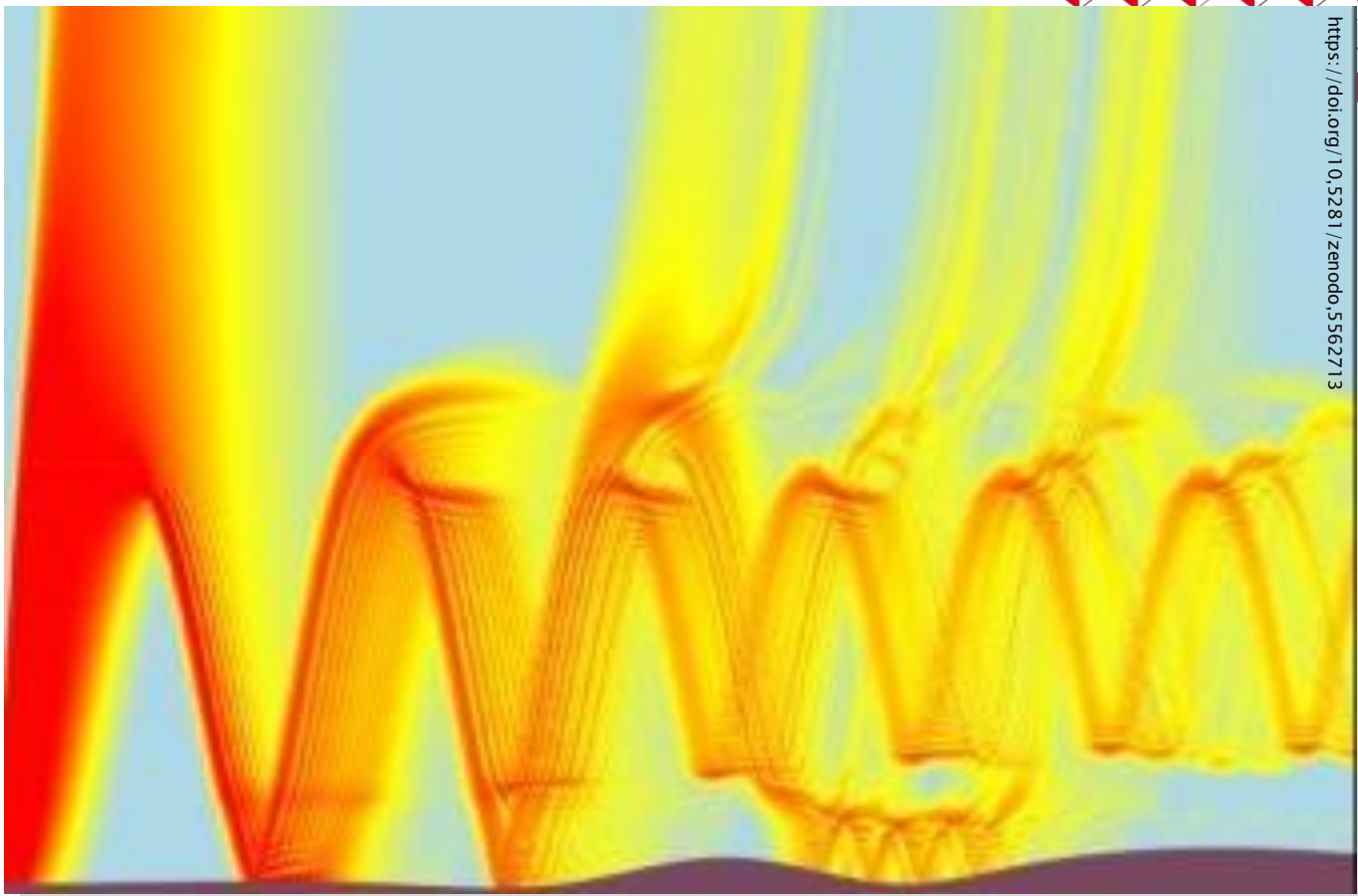
¹ CEA/DAM/DIF, F-91297, Arpajon, France

² IRD, Sorbonne Université, UMMISCO, F-93143, Bondy, France

³ THEMA, CY Cergy Paris université, F-95011, Cergy-Pontoise, France

⁴ LIRIS, Université Lyon 1, F-69130, Ecully, France

*In collaboration with NORSAR, Norway
BRISSAUD Quentin, NÄSHOLM Sven Peter*



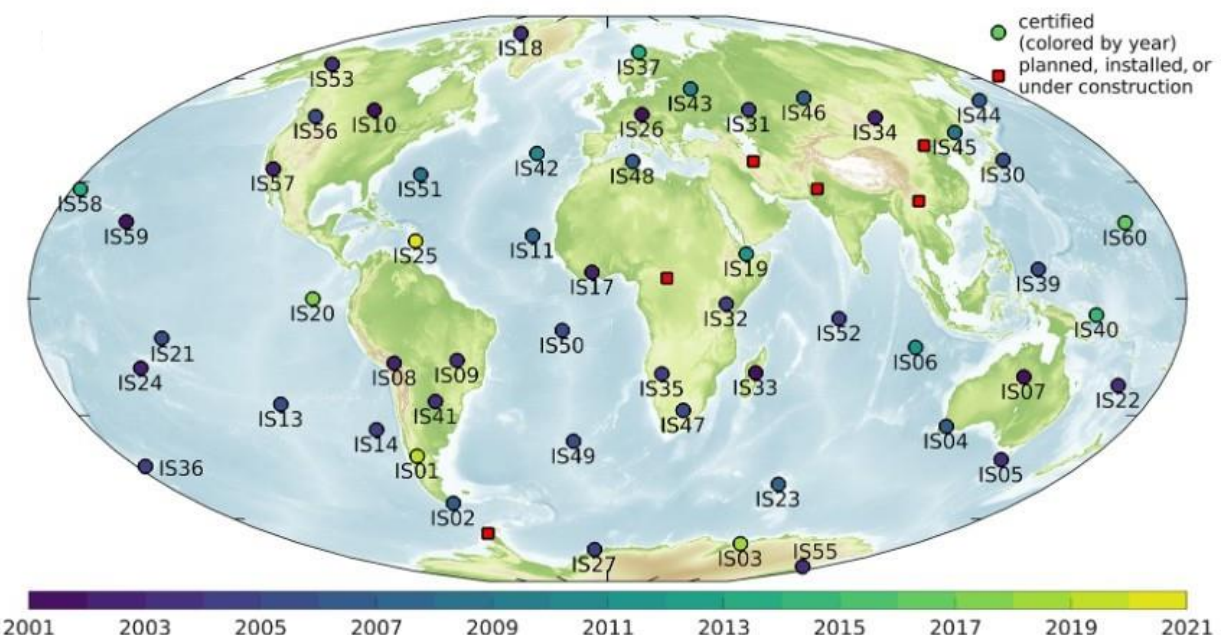
<https://doi.org/10.5281/zenodo.5562713>



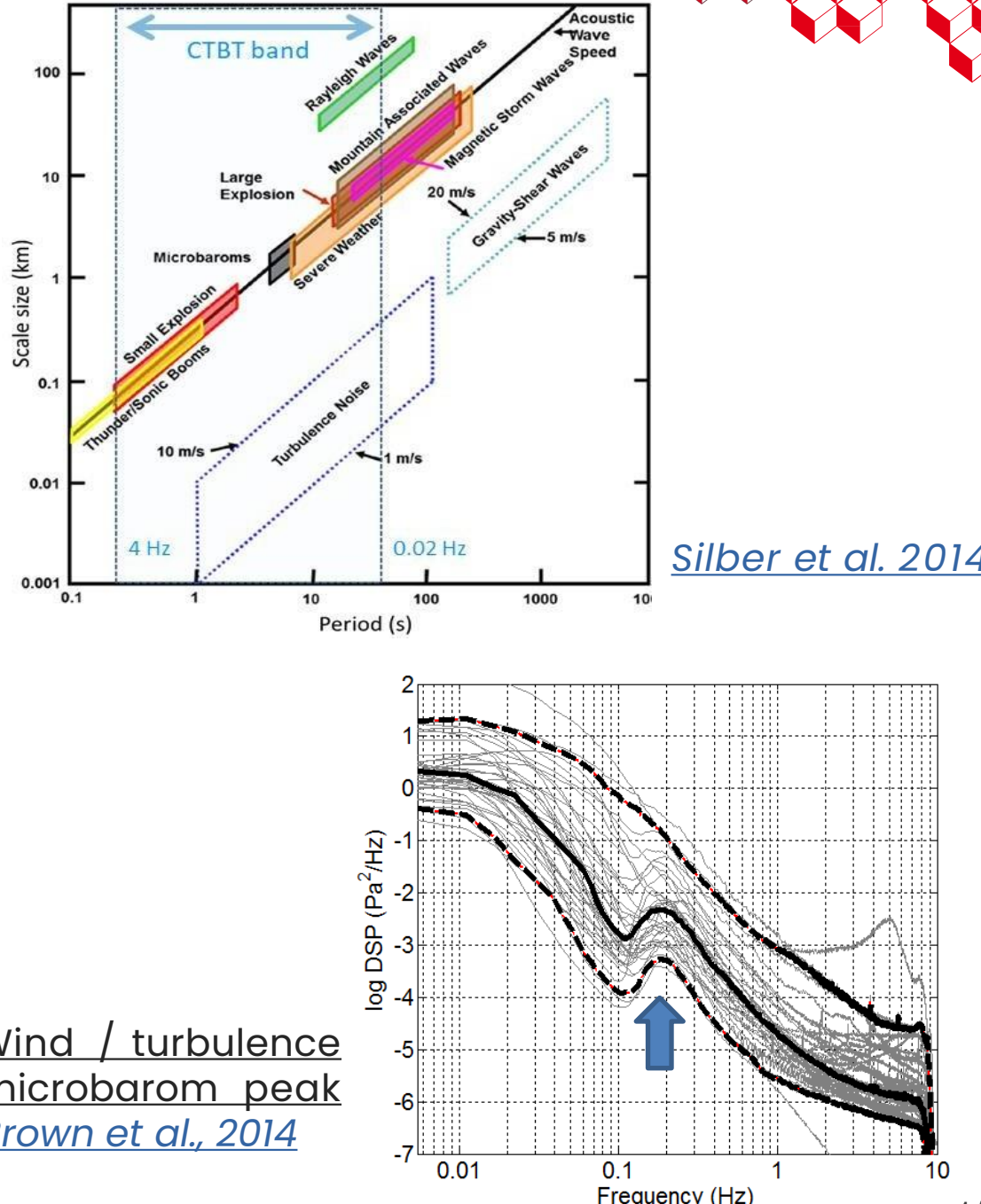


Context: CTBT

- International Monitoring System (IMS) under the Comprehensive Nuclear Test Ban Treaty (CTBT)
- infrasound stations uniformly distributed around the globe to detect, characterize and locate 1kt nuclear explosions
- Many sources; natural (volcanoes, earthquakes, etc.) or artificial (turbines, explosions, etc.)



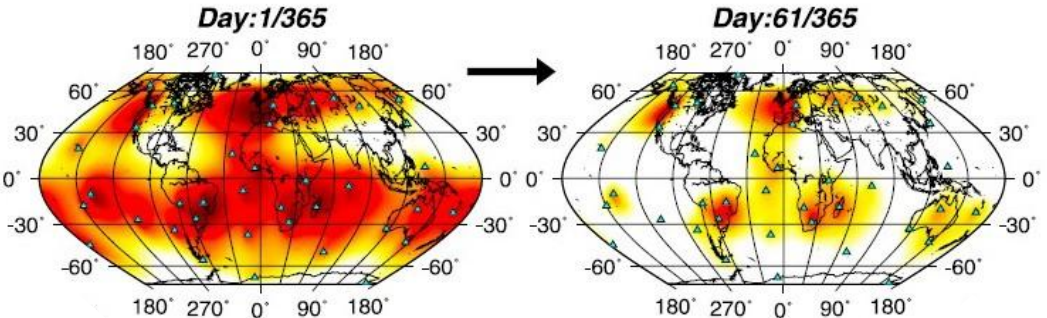
Overview of the IMS infrasound network
[\(Hupe et al. 2021\)](#)



Wind / turbulence
microbarom peak
[Brown et al., 2014](#)

Motivations

- Assess IMS detection capabilities: requires near-real-time modeling of infrasound transmission losses (TLs)
- Existing full wave propagation modeling tools (used to model TLs): costly
- *Brissaud et al. 2023*: deep learning algorithm to model TLs up to 1,000 km in near-real-time

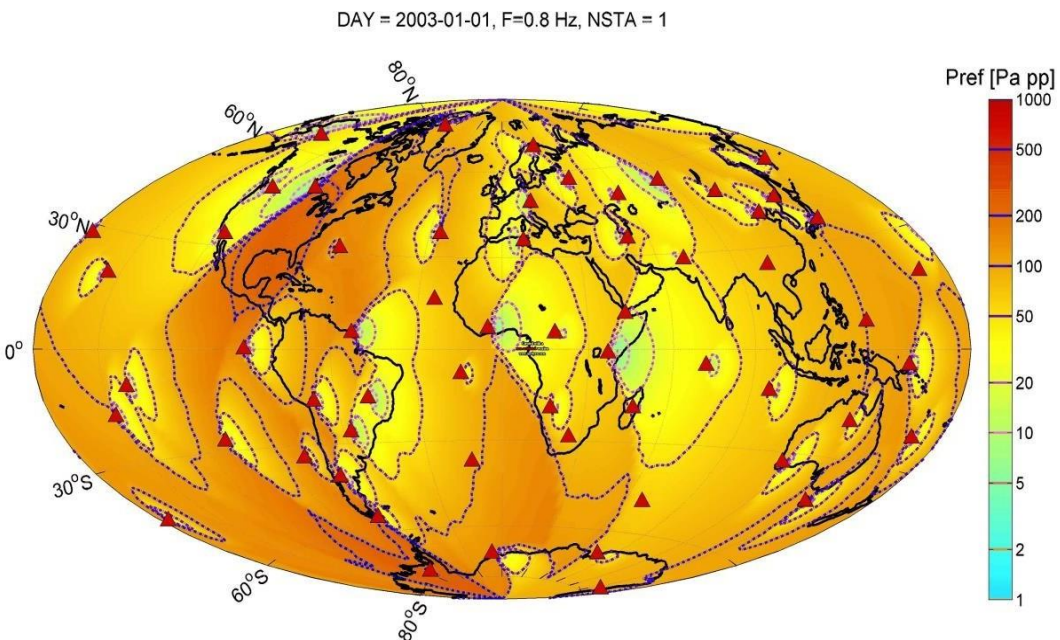


Detection capability of IMS: highly variable in space and time (90 % detection probability) ([Green et al. 2010](#))



Objectives

- accurate + near-real-time modeling of TLs up to 4,000 km;
- quantify associated uncertainties;
- account for the multiple atmospheric range-dependent wave guides.
- draw IMS detectability maps in near real-time
using deep learning



IMS capacity of detection map at 0,2 Hz



Method

From realistic 2D range-dependent atmospheric slices...

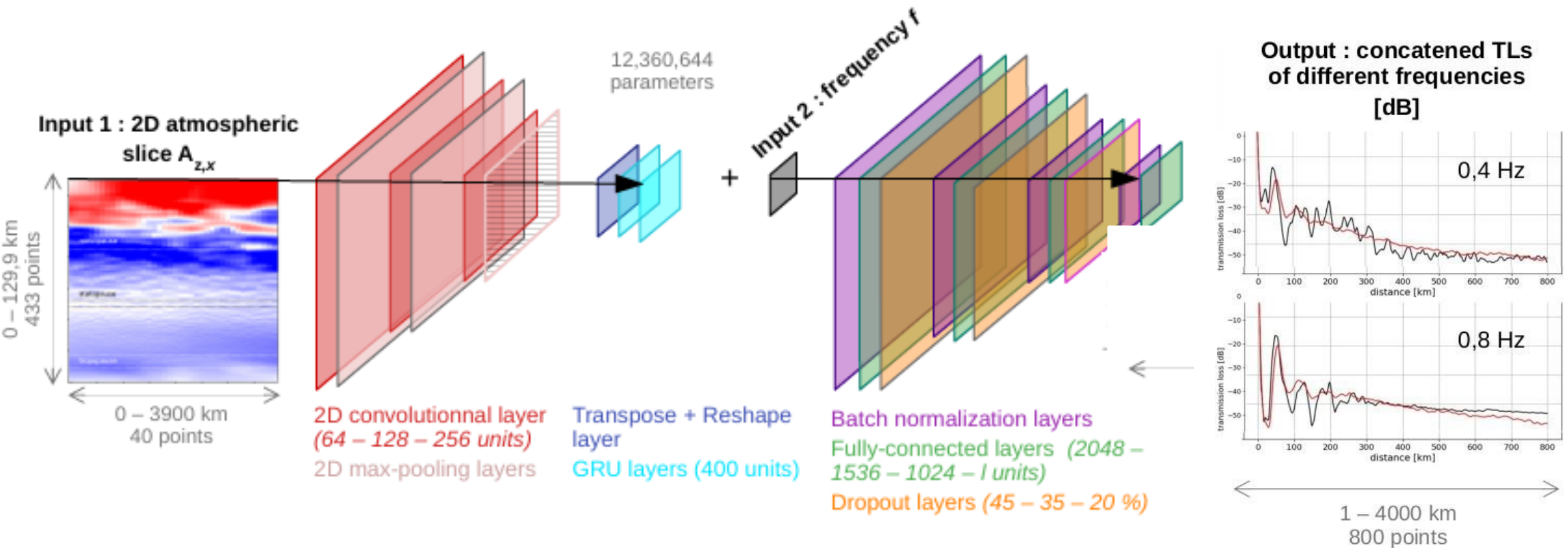
... using a Convolutional Recurrent Neural Network

... estimate in near-real-time ground-level TLs up to 4,000 km at \neq frequencies

inputs

method

outputs





Inputs: atmospheric slices

- **Realistic range-dependent 2D atmospheric slices at a global scale**

- Mean atmospheric conditions

$x \in [0; 4,000]$ km distance;

$z \in [0; 130]$ km altitude;

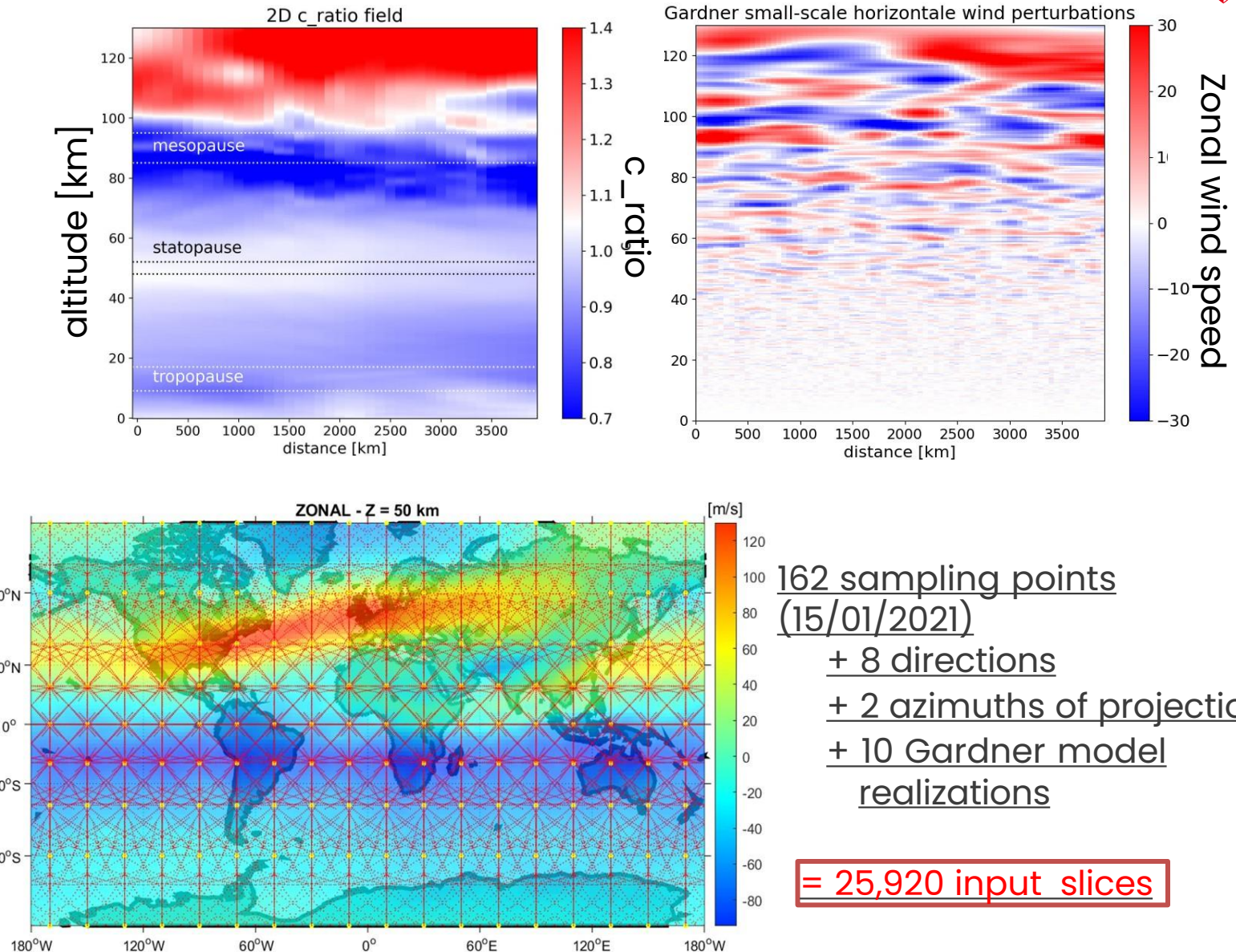
vertical temperatures + horizontal windspeeds extracted using the Whole Atmosphere Community Climate Model ([Gettelman et al. 2019](#)).

- Small scale variations

partly due to gravity waves;

small-scale windspeed perturbations ([Gardner et al. 1993](#))

Atmospheric slice + small scale variations



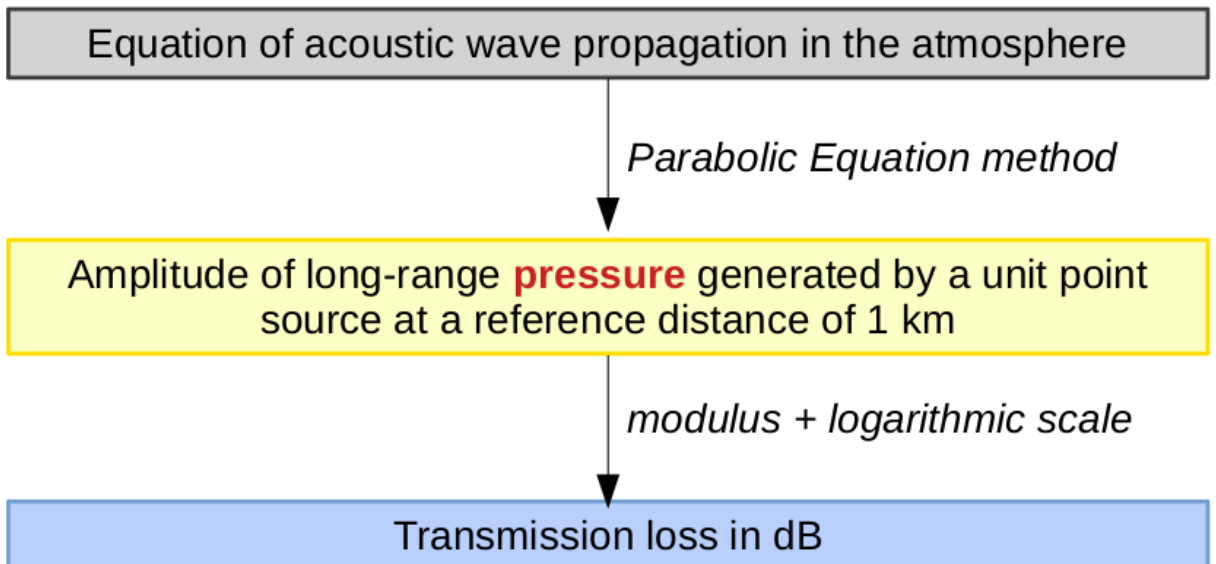


Output: transmission losses

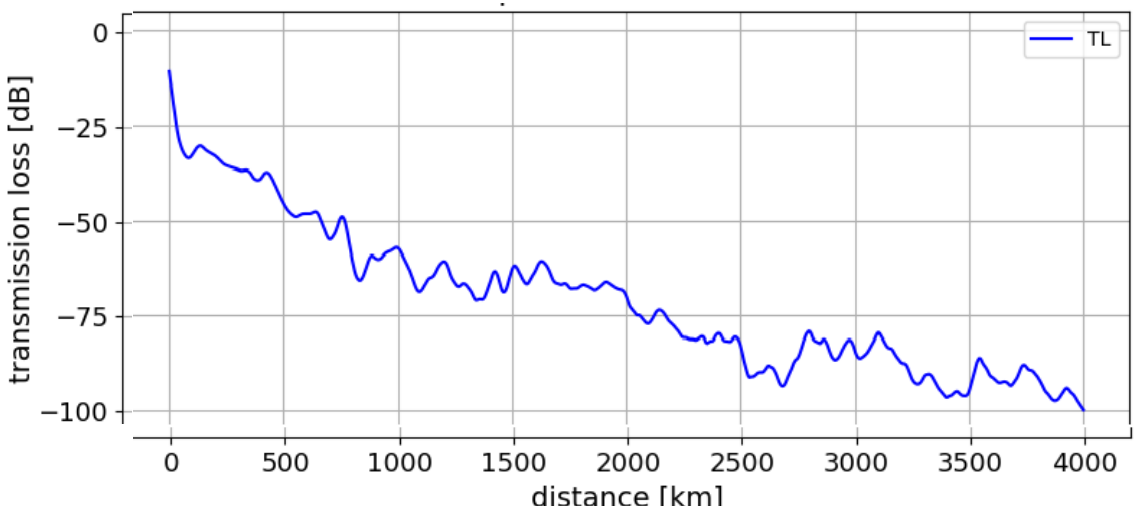
- **Ground-level infrasound TLs**

- $x \in [0; 4,000]$ km distance
- Atmospheric absorption coefficients (*Sutherland et al. 2004*)
- Parabolic equation (PE) solver (*Waxler et al. 2021*)
- 5 frequencies: 0.1, 0.2, 0.4, 0.8 and 1.6 Hz.

→ 25,920 slices x 5 = 129,600 simulations



PE simulation at 0.2 Hz



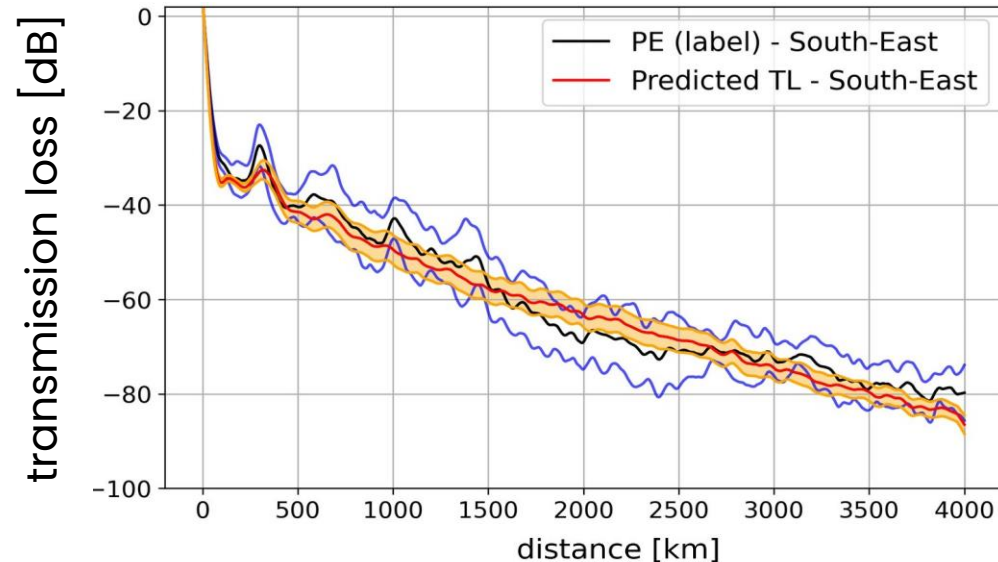
Results: training + testing performances

- **Training process**

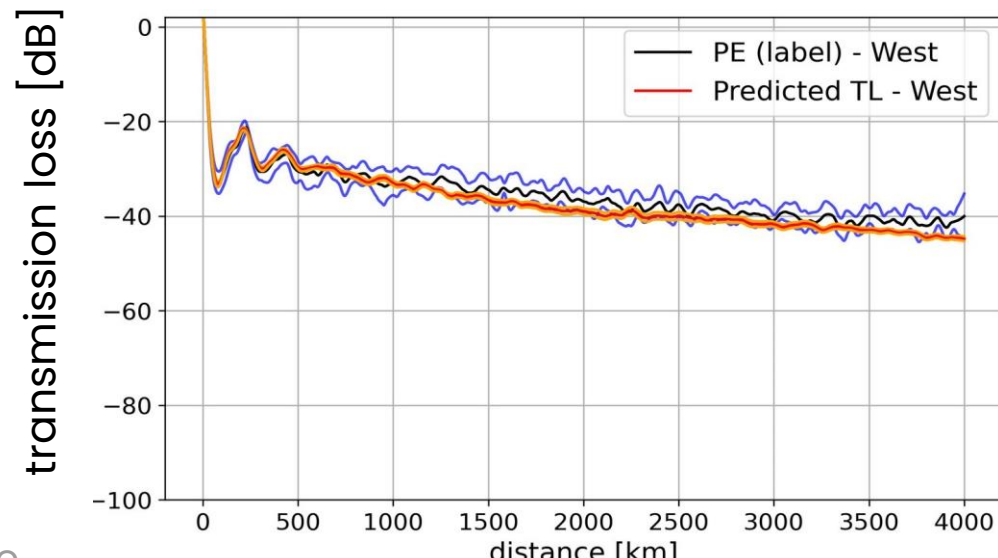
- On A100 GPU
- convergence of the model after 30 iterations (~ 7s / iteration)

- **Test performances**

- Good estimation of mean attenuation + asymptotic behavior over 4,000 km
- Small-scale variations not fully recovered
- Robust in all initial atmospheric scenarios



Predicted TLs / expected PE
0.2 Hz
No stratospheric duct



Predicted TLs / expected PE
1.2 Hz
Stratospheric duct



Results: error metrics

- Mean Relative Absolute Error (**MRAE**): difference in %

median of 7.5 % over 4,000 km;

> 15 % generally below 200 km distance.

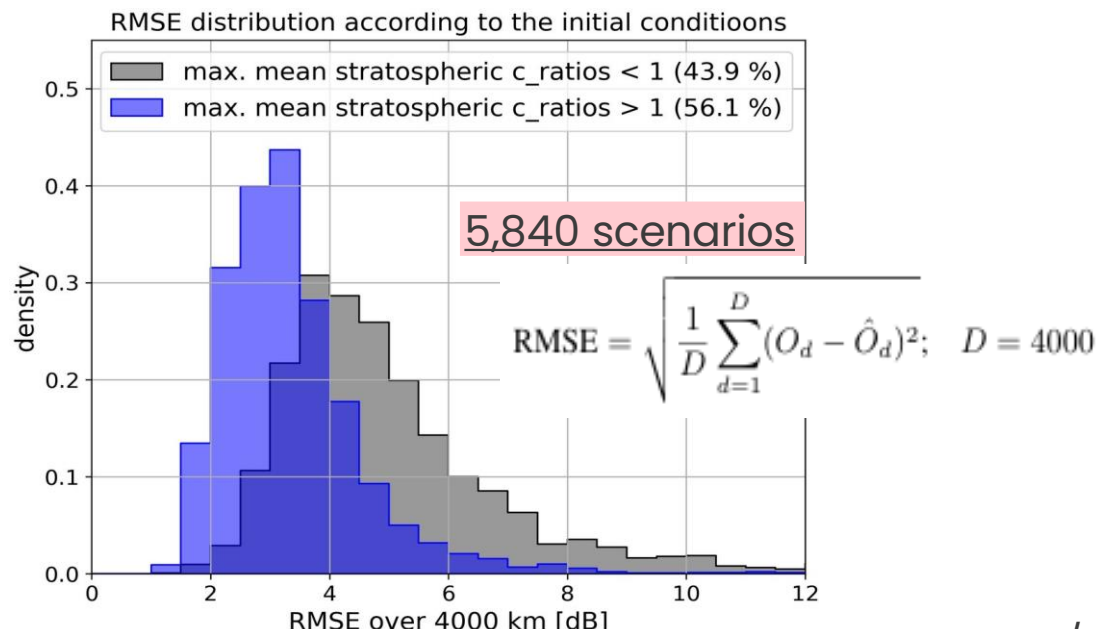
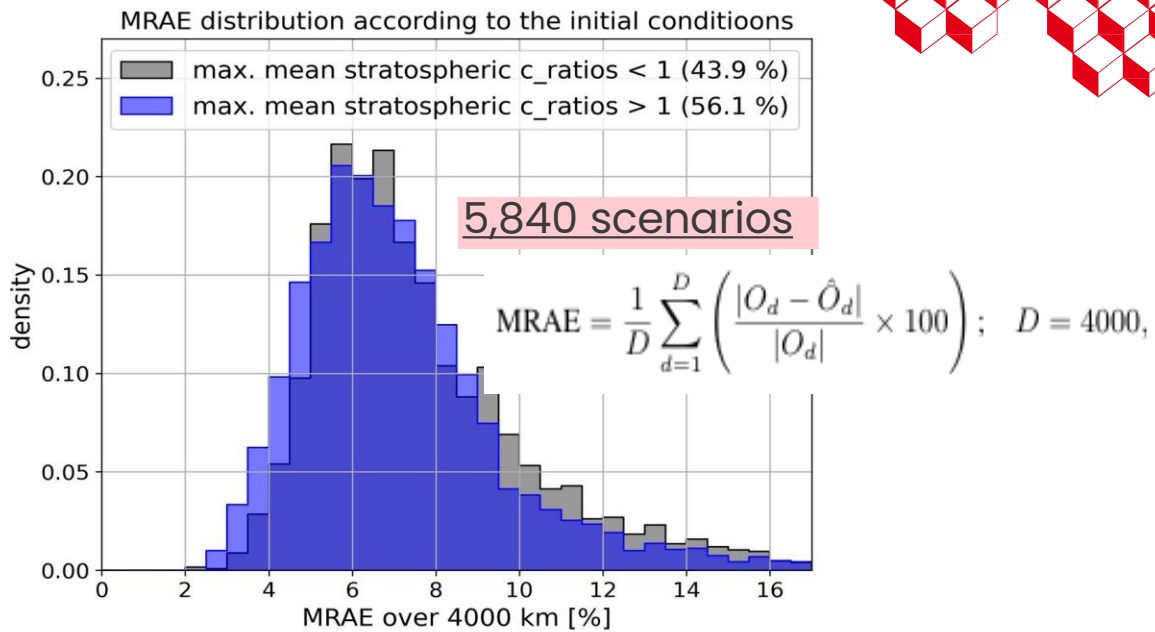
- Root Mean Squared Error (**RMSE**): difference in dB

median of 4 dB over 4,000 km;

higher mean RMSE of ~1 dB for scenarios without stratospheric wave duct.



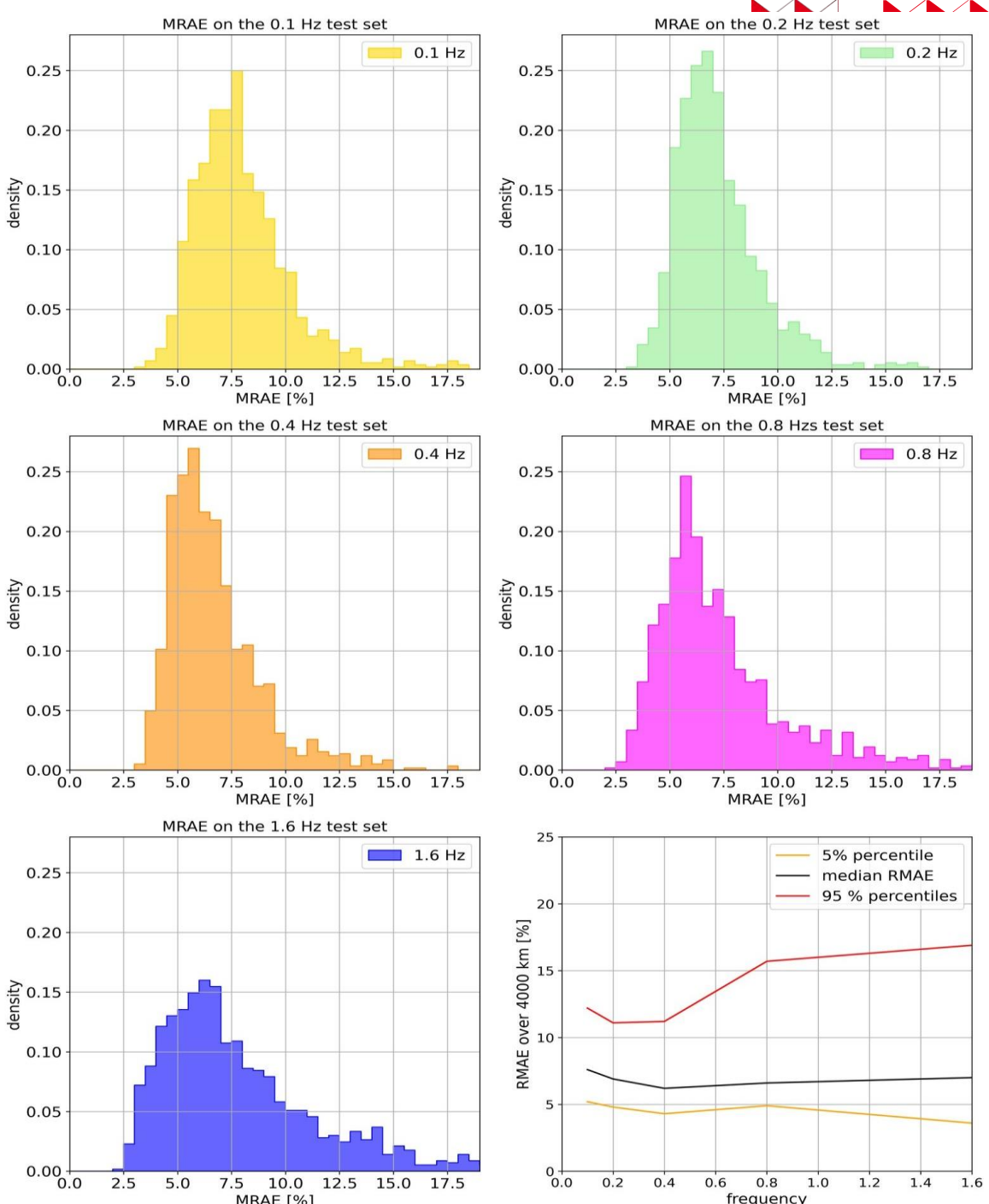
→ consistent with Brissaud et al. 2023: mean RMSE of 5 dB regardless of the initial conditions over 1,000 km



Results: « frequency effect »

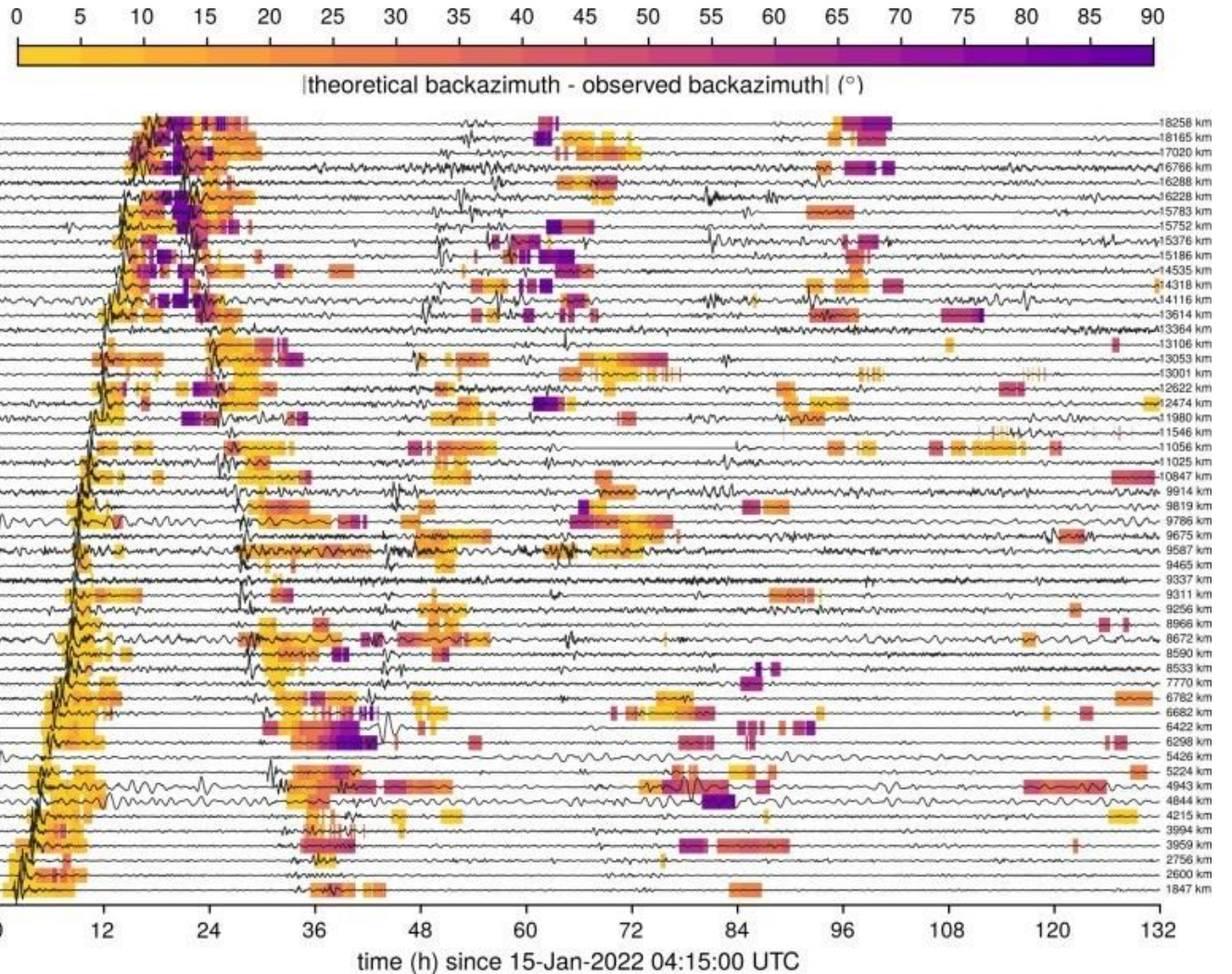


- Degradation of performance with increasing frequencies
 - identical median of 7,5 % RMAE for the 5 frequencies;
 - higher 95 % percentile for higher frequencies.



Results: generalization performances

- Generalization set : atmospheric slices around the Tonga Volcano (01/15/22)
→ different from the training slices
- Estimate attenuation maps around the volcano, obtained almost instantaneously (~ 0,05 s / prediction)

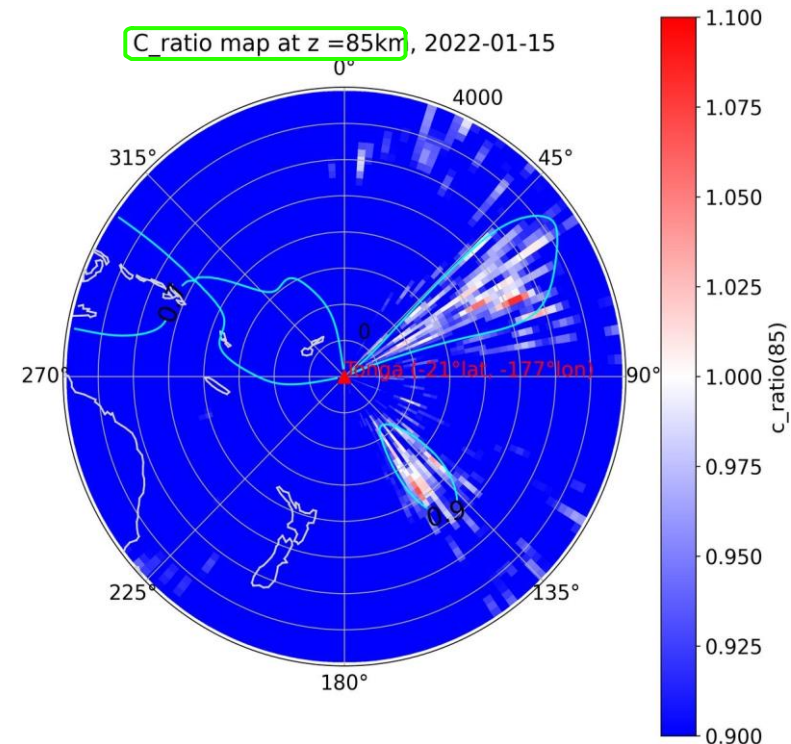
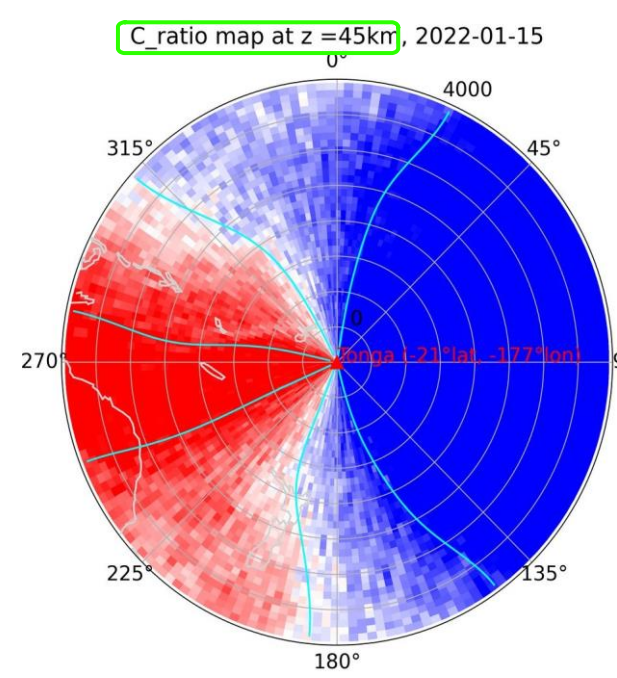
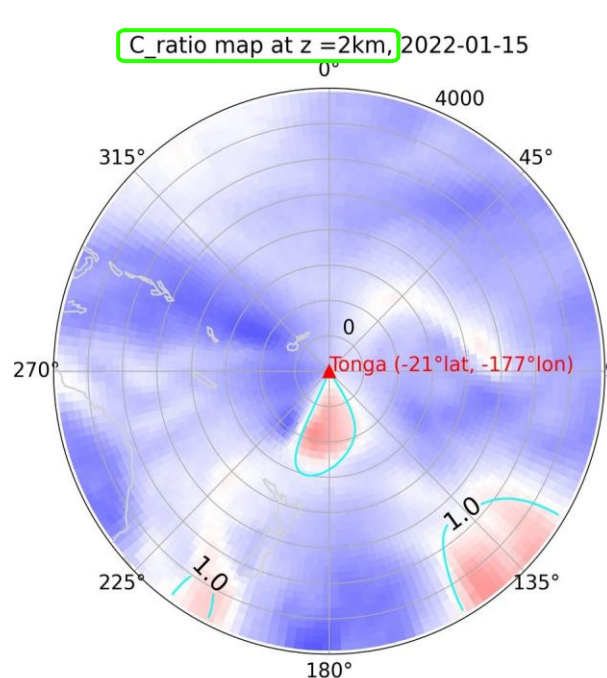


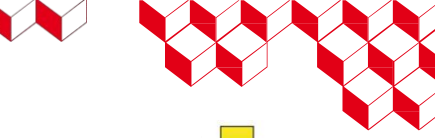
Infrasound detection on the entire surveillance network ([Vergoz et al. 2022](#))



Results: generalization inputs

Atmospheric conditions that day

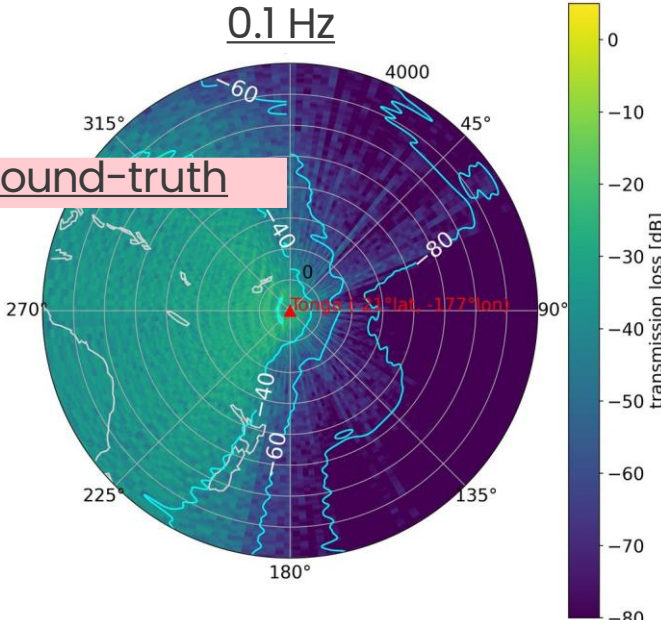




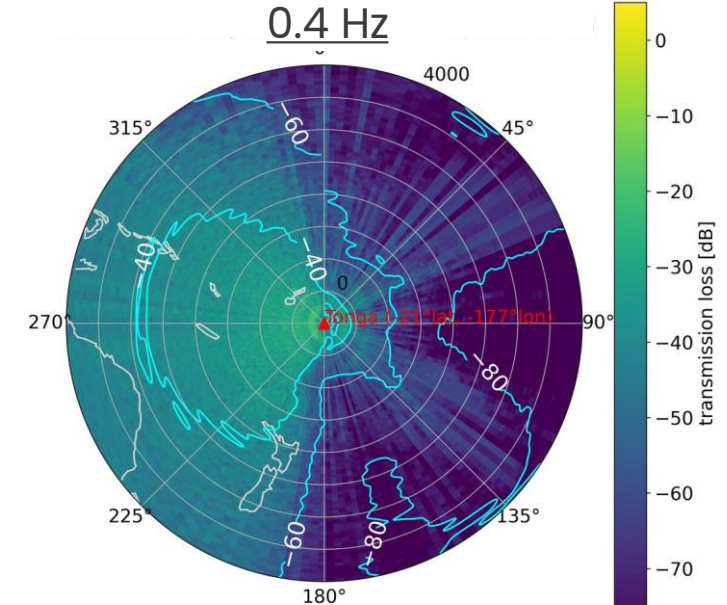
Results: generalization

0.1 Hz

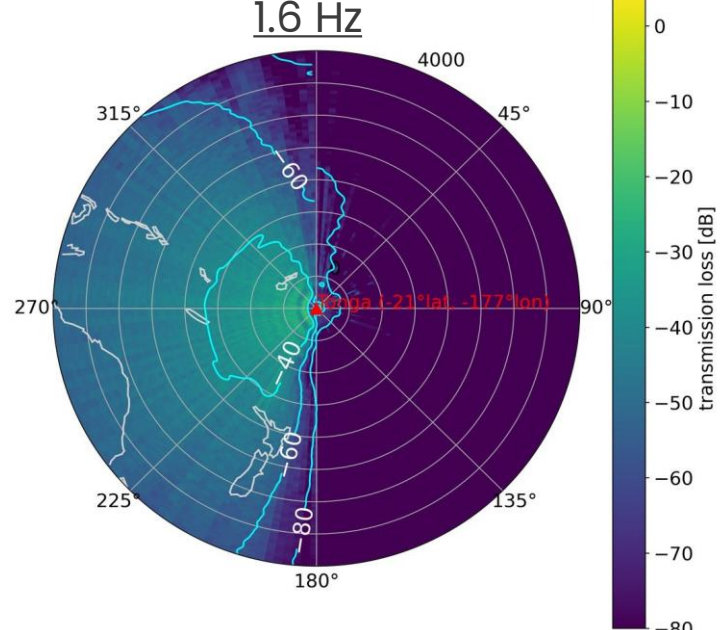
Ground-truth



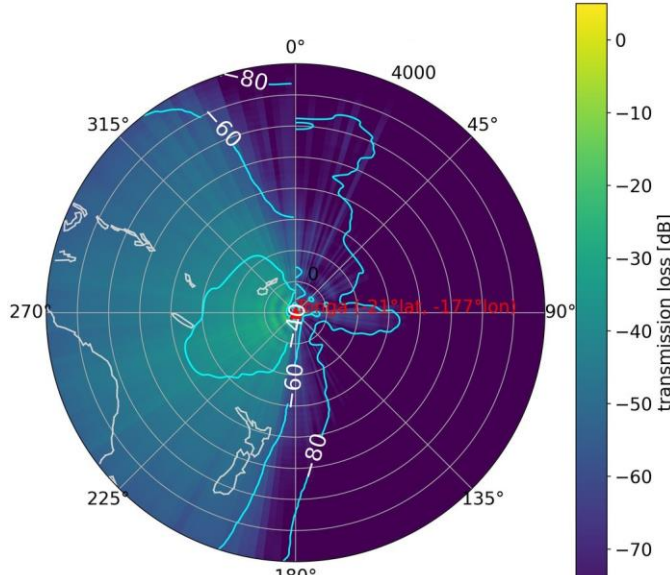
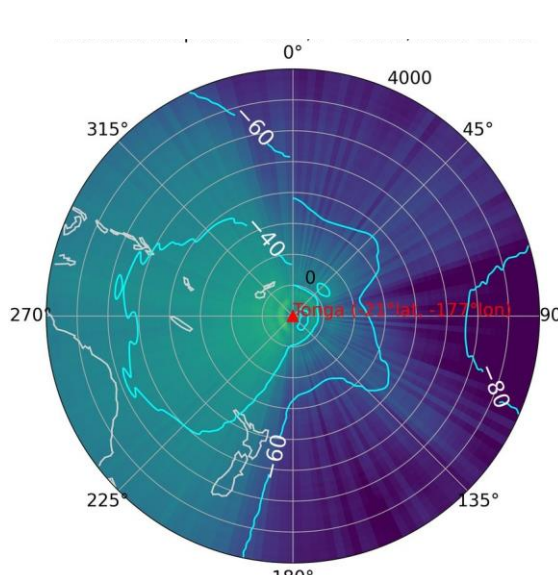
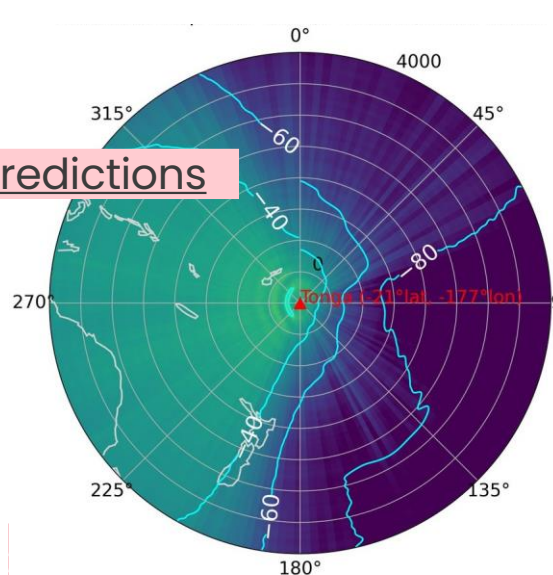
0.4 Hz



1.6 Hz



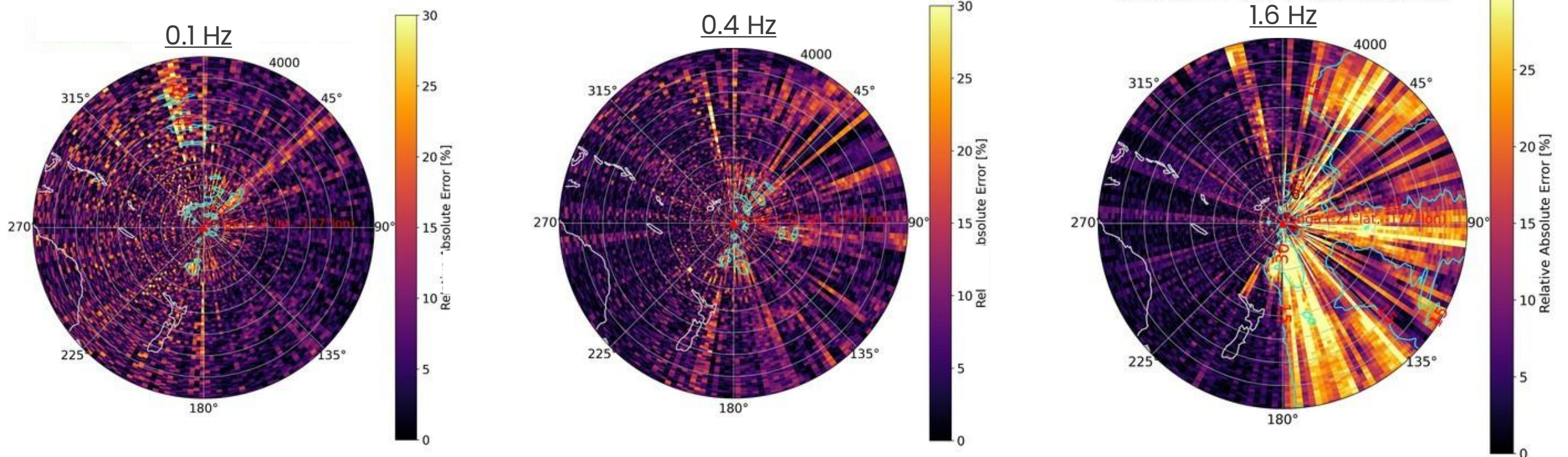
Predictions





Results: generalization errors

Point-by-point Relative Absolute Error (%) between predictions / expected TLs

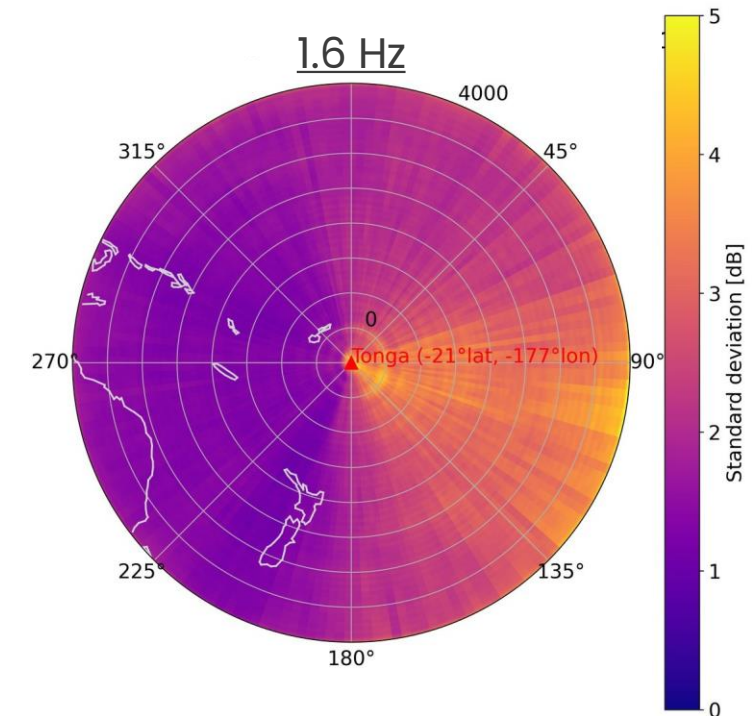
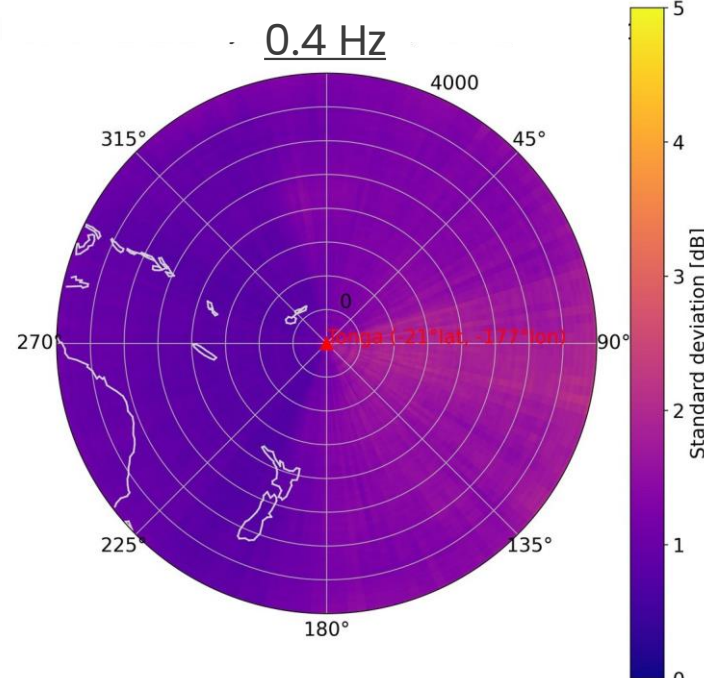
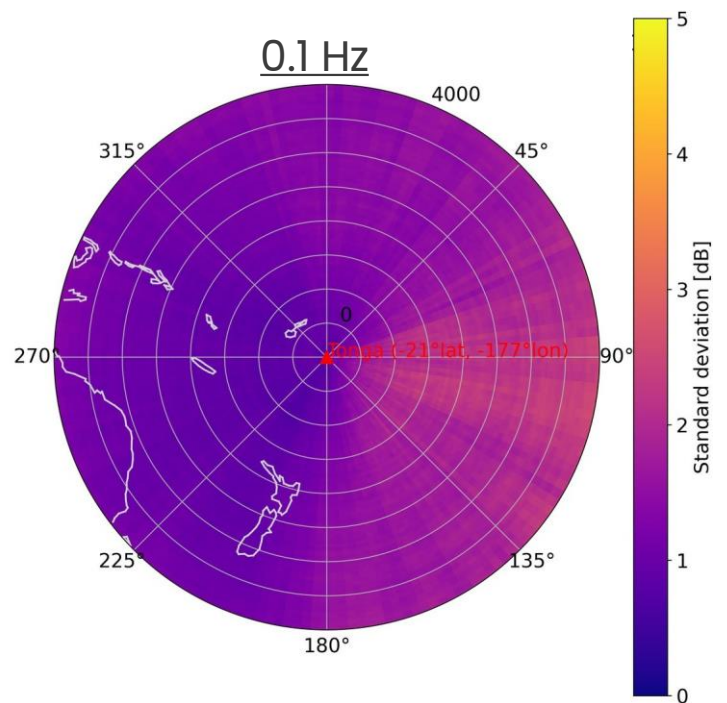


$$\text{RAE} = \frac{|\text{label}_d - \text{pred}_d|}{\text{label}_d} \times 100 \quad ; \quad d \in [1, 4000]$$



Results: generalization uncertainty

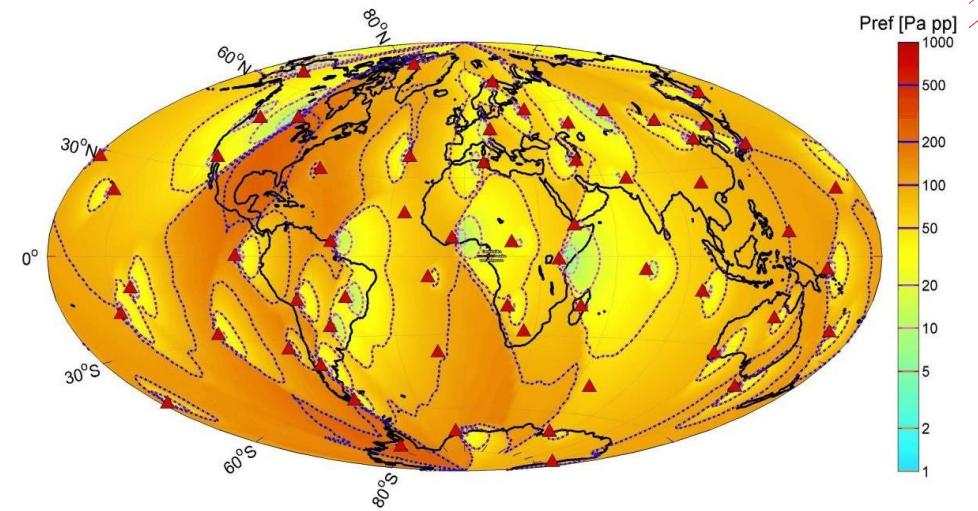
Model + data uncertainty associated with predictions *(Gawlikowski et al. 2023)*



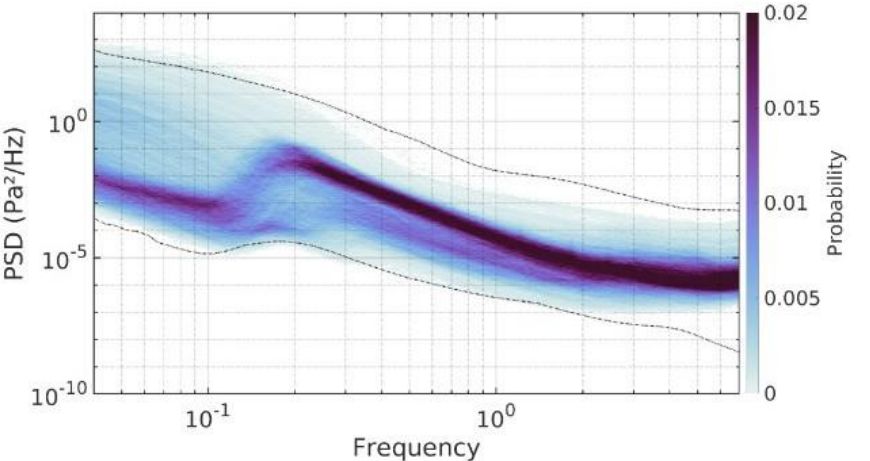
Summary / perspectives

- 1st surrogate deep learning model mapping 2D realistic atmospheric
 - slices with ground-level TLs at \neq frequencies Confidence levels: model + data uncertainty
 - Promising results using global dataset (WACCM, winter time): testing $\approx 7.5\%$ and generalization $\approx 10\%$ of MRAE over 4000 km
 - Ongoing evaluation on reference events (global and regional scales)
-
- **Perspectives**
 - Enlarge training dataset: spatial / time coverage
 - Ensemble Prediction System (Integrated Forecasting System)
 - Global detection capability maps using measured station noise
 - Develop **Transformer** architectures (*Vaswani et al. 2017*):
 - improve the encoding of atmospheric and propagation conditions capture;
 - more effectively complex range-dependent features;
 - recover small scale atmospheric variations.

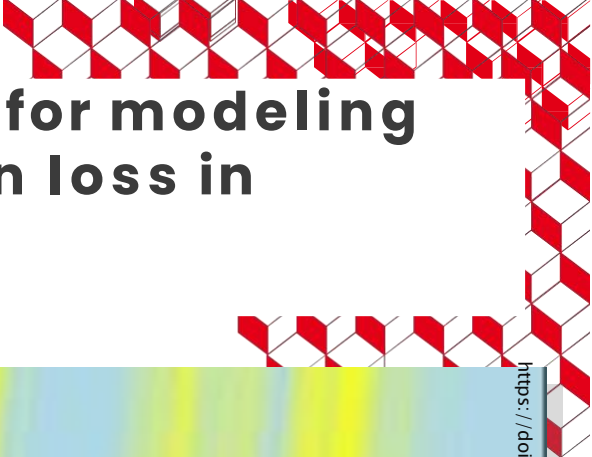
DAY = 2003-01-01, F=0.8 Hz, NSTA = 1



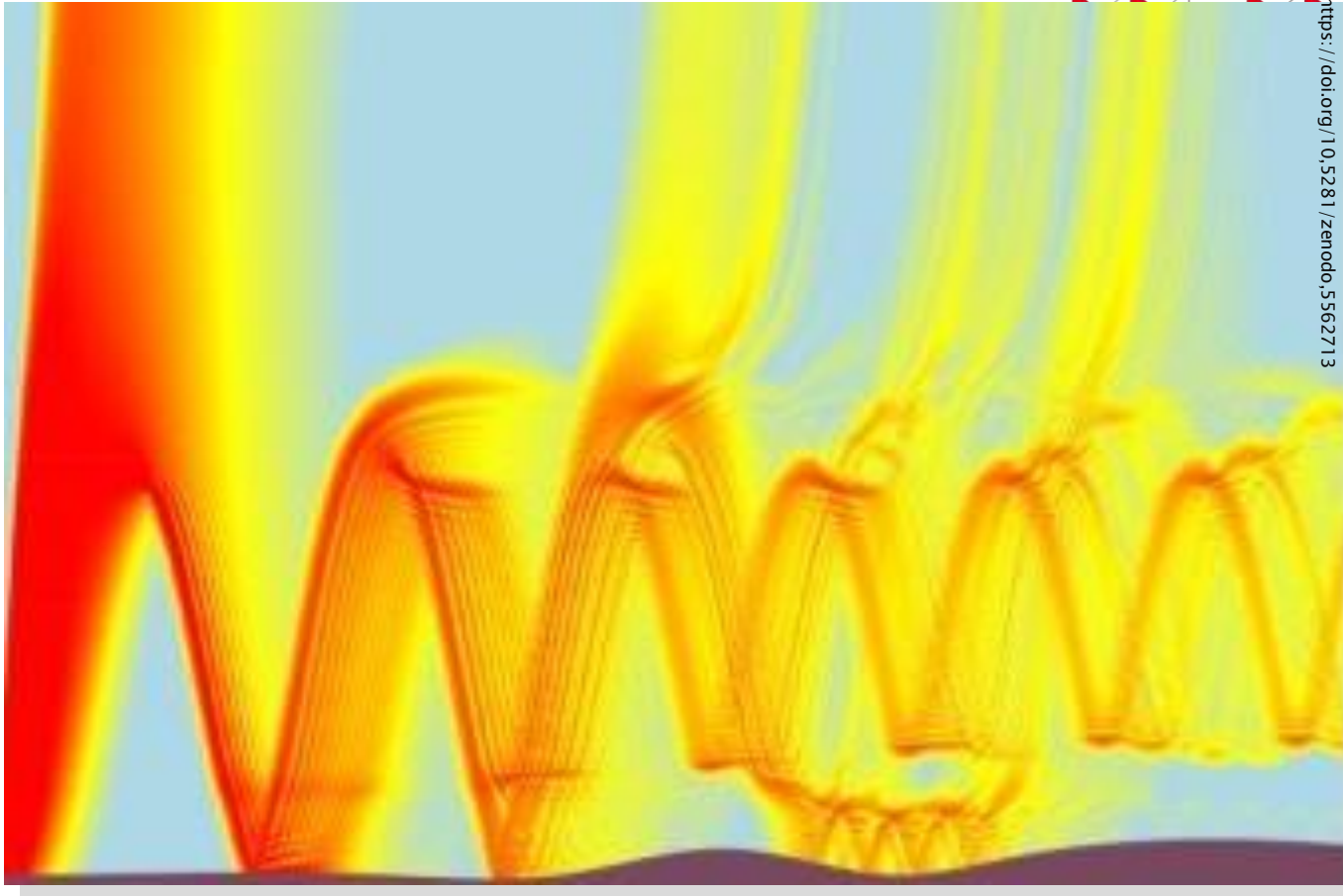
IMS capacity of detection map at 0.2 Hz



PSD probability density at IS37 infrasound station



Deep learning methods for modeling infrasound transmission loss in the middle atmosphere



<https://doi.org/10.5281/zenodo.5562713>

cea



LIRIS

Thank you for your attention !





Selected references

- Green, D.N. et al. (2010). Journal of Geophysical Research: Atmospheres, 115(D18).
- Le Pichon et al. (2012), Incorporating numerical modeling into estimates of the detection capability of the IMS infrasound network, Journal of Geophysical Research, 117, <https://doi.org/10.1029/2011JD016670>
- Brissaud, Q. et al. (2022). Predicting infrasound transmission loss using deep learning, Geophysical Journal International, 232(1), 274–286.
- Gardner, C.S. et al. (1993). Journal of Geophysical Research: Atmospheres, 98(D1), 1035–1049.
- Sutherland, L. C., & Bass, H. E. (2004). Atmospheric absorption in the atmosphere up to 160 km. The Journal of the Acoustical Society of America, 115(3), 1012–1032.
- Assink, J., Waxler, R. (2019), Propagation modeling through realistic atmosphere and benchmarking, Infrasound monitoring for atmospheric studies, In: Le Pichon A, Blanc E, Hauchecorne A (eds) Infrasound monitoring for atmospheric studies: 2nd ed. Springer Nature, Dordrecht, ISBN: 978-3-319-75140-5, 509–549.
- Marty et al. (2021), Low and High Broadband Spectral Models of Atmospheric Pressure Fluctuation, Journal of Atmospheric and Oceanic Technology 38, DOI:10.1175/JTECH-D-21-0006.1
- Gawlikowski, et al. (2023). A survey of uncertainty in deep neural networks. Artif. Intell. Rev. 56, <https://doi.org/10.1007/s10462-023-10562-9>
- Vaswani, A. (2017). Attention is all you need. Advances in Neural Information Processing Systems.

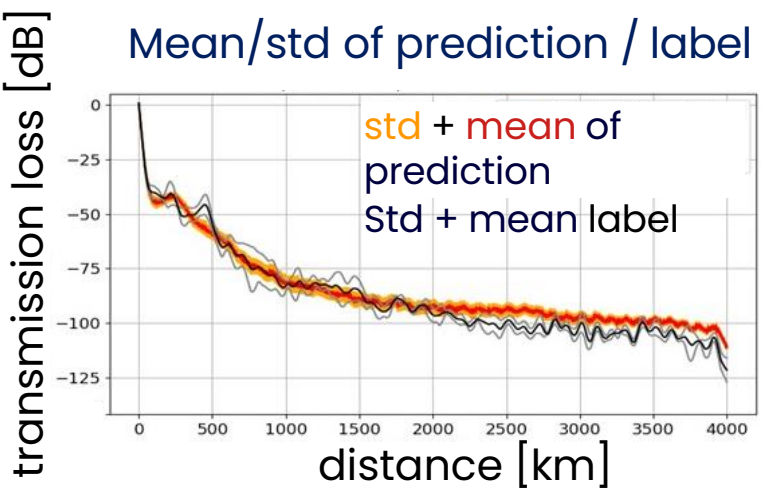
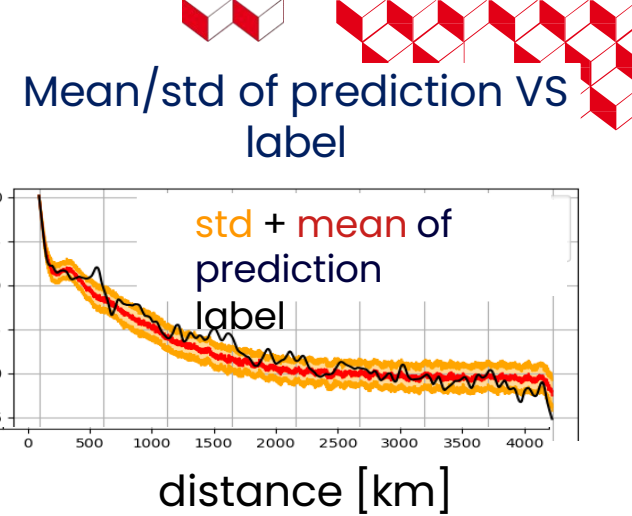
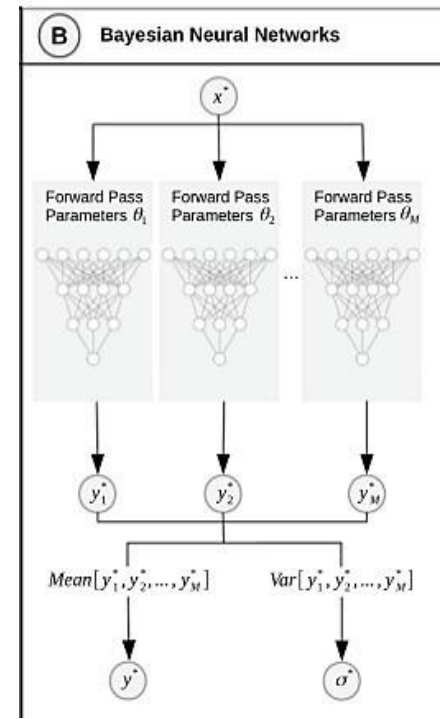


Selected references

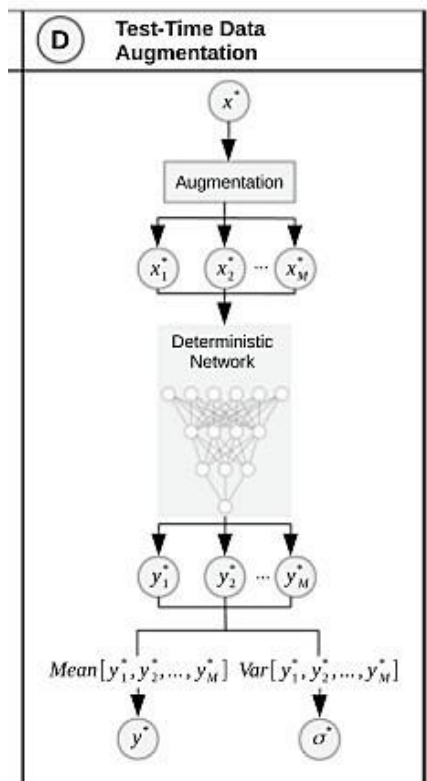
- Sabatini R. (2017), Simulation directe 3-D de la propagation non linéaire des ondes acoustiques dans l'atmosphère terrestre, Doctorat Ecole Centrale Lyon, <https://www.theses.fr/2017LYSEC004>
- Vergoz, J., Hupe, P., Listowski, C., Le Pichon, A., Garcés, M. A., Marchetti, E., ... & Mialle, P. (2022). IMS observations of infrasound and acoustic-gravity waves produced by the January 2022 volcanic eruption of Hunga, Tonga: A global analysis. *Earth and Planetary Science Letters*, 591, 117639. <https://doi.org/10.1016/j.epsl.2022.117639>
- Hupe, P., Ceranna, L., Le Pichon, A., Matoba, R. S., and Mialle, P.: International Monitoring System infrasound data products for atmospheric studies and civilian applications, *Earth Syst. Sci. Data*, 14, 4201–4230, https://doi.org/10.5194/essd-14-4201-2022_2022.
- Brown, D., Ceranna, L., Prior, M. et al. The IDC Seismic, Hydroacoustic and Infrasound Global Low and High Noise Models. *Pure Appl. Geophys.* 171, 361–375 (2014). <https://doi.org/10.1007/s00024-012-0573-6>

uncertainty + sensitivity

- **Model uncertainty : Bayesian method (Monte-Carlo Dropout)**
 - Make dropout layers active during training + predicting stages
 - Make the model no more deterministic but stochastic
 - m TLs predictions realized from each test-data → **mean** and **std** (= uncertainty) computed
- **Data sensitivity : Test-Time Augmentation**
 - Each test-data is augmented in m versions using \neq Gardner realizations
 - Prediction of m TLs → **mean** and **std** computed + compared to mean and std of expected labels



Gawlikowski et al. 2023



Training set VS generalization set

